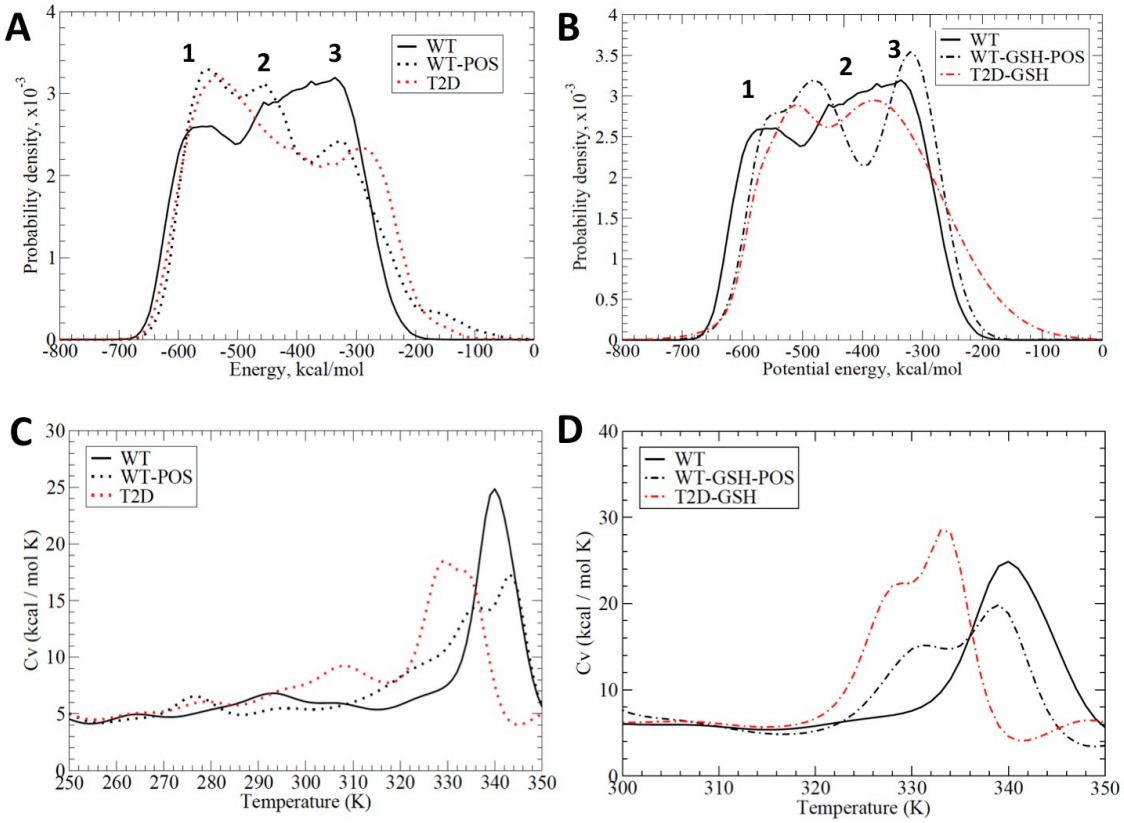

Figure S1, related to Figure 1. T2D-SOD1 reproduces the biophysical properties of T2-phosphorylated SOD1 in DMD simulations. Comparison of the wild type SOD1 (WT, black line), T2-phosphorylated SOD1 (WT-POS, black dot) and T2D-SOD1 (T2D, red dot) for their potential energy distributions (A) and specific heat (C). The same comparison is made for C111-glutathionylated SOD1 (B and D).

Figure S2, related to Figure 1. Crystal packing of T2D in P1 space group. Central dimers are shown in green and cyan.

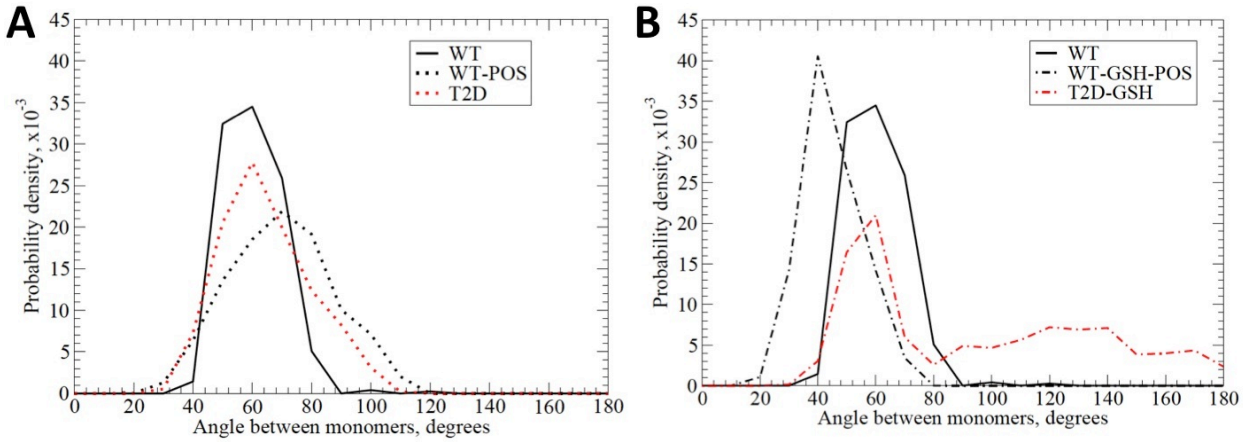

Figure S3, related to Figure 1. DMD simulations demonstrate that T2D-SOD1 and P_i-SOD1 feature larger monomer-monomer angles on average, as compared to WT-SOD1.

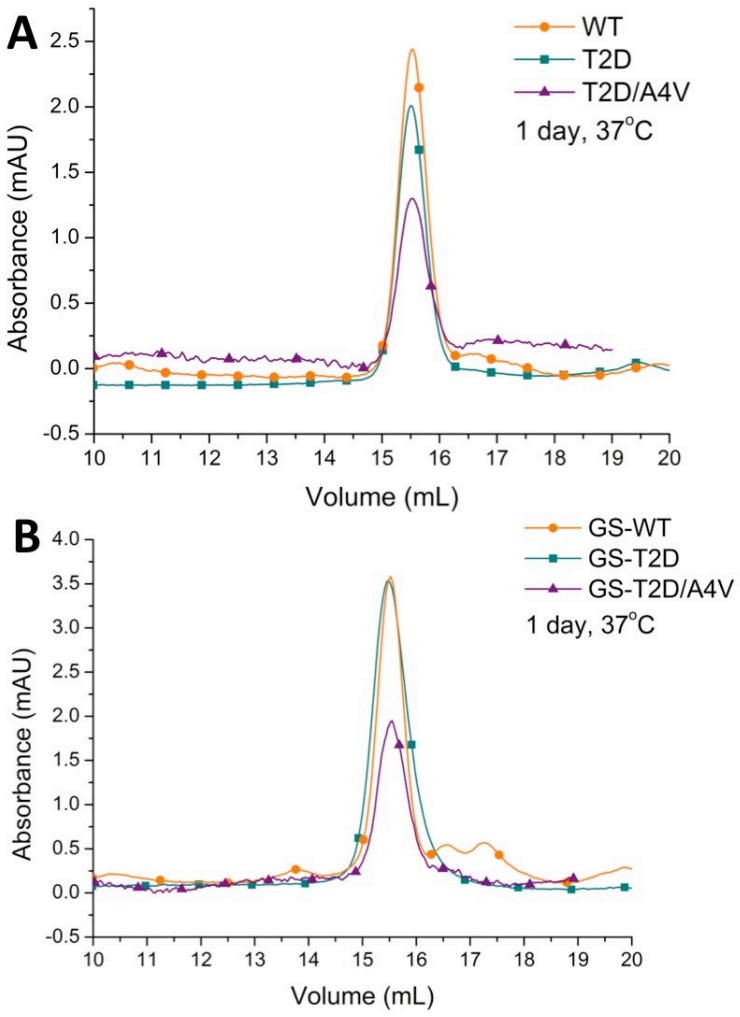

Figure S4, related to Figure 2. Time resolved size exclusion chromatograms for unmodified T2D-, T2D/A4V- and WT-SOD1 (A) and glutathionylated proteins (B). Samples were taken after incubation at 37°C for one day. T2D-SOD1 and T2D/A4V-SOD1 feature increased stability of dimeric population as compared to unmodified species or glutathionylated species.

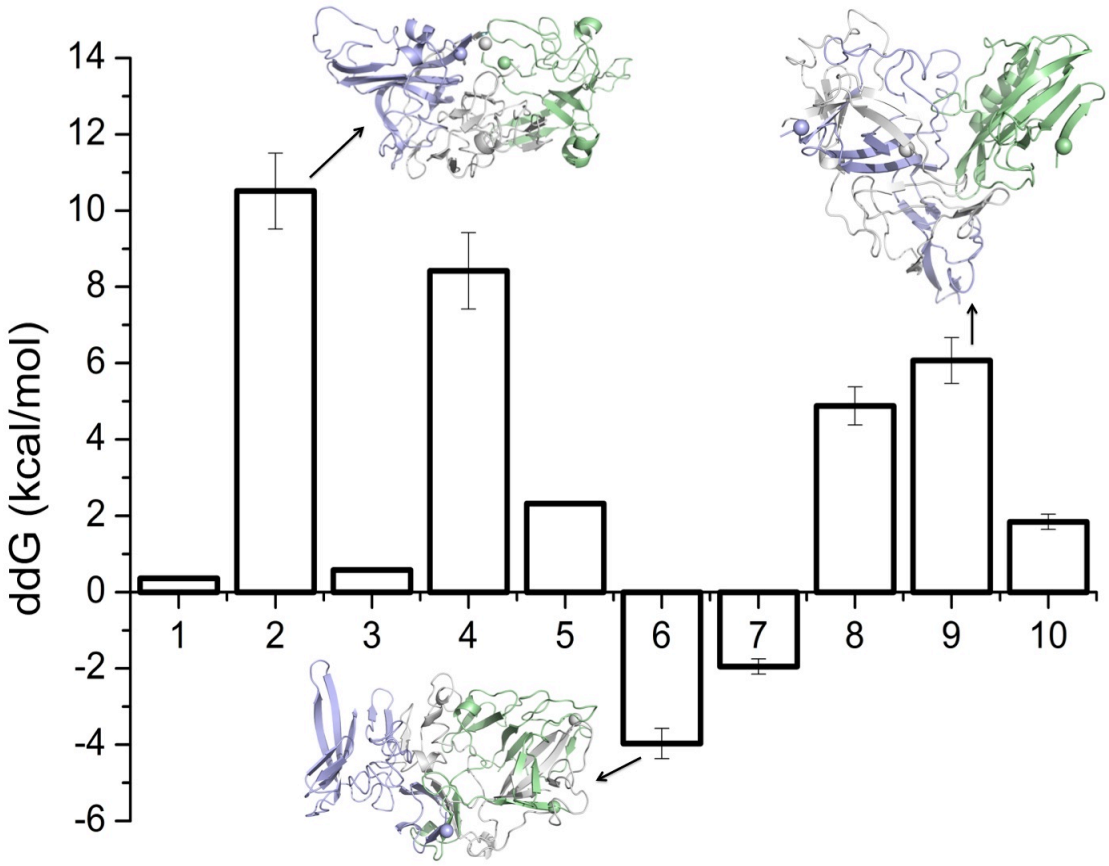

Figure S5, related to Figure 4. T2D mutation destabilizes SOD1 trimer. Calculations were performed on ten trimer structural models (Proctor et al., 2016). The T2D mutation significantly destabilizes trimer models 2, 4, 8, and 9 (positive ΔΔG). It stabilizes trimer model 6 and 7 (negative ΔΔG). The average ΔΔG is 2.9 kcal/mol ± 0.4 kcal/mol. Representative trimer models with the highest and lowest ΔΔG are shown with the position of D2 represented as spheres.

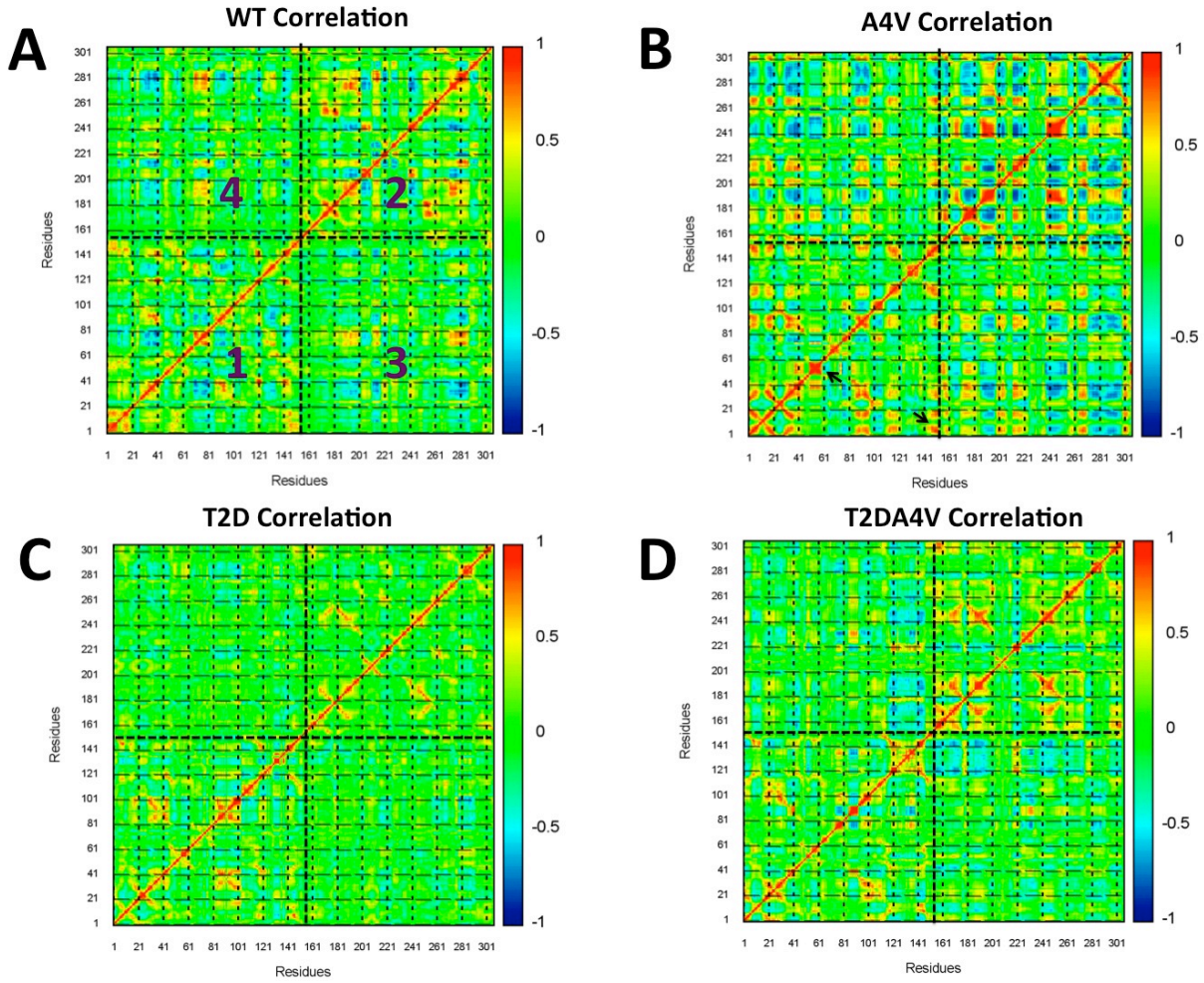

Figure S6, related to Figure 4. **Covariance matrices of wild type SOD1 and mutants**: (A) WT-SOD1, (B) A4V-SOD1, (C) T2D-SOD1 and (D) T2D/A4V-SOD1. A4V-SOD1 has a larger number of long-range positively correlated (red) and negatively correlated (blue) residue motions as compared to other constructs. Squares 1 and 2 represent the correlations within the two monomers, and 3 and 4 represent the correlations between the monomers, respectively. The cross-correlated regions (residue 40-50, 146-150) are indicated with black arrow in the plot of A4V-SOD1. The results are an average of ten DMD trajectories. Cross-correlation maps are calculated as in (Khare and Dokholyan, 2006).

Aggregation propensity of T2D-SOD1: We have applied TANGO (Fernandez-Escamilla et al., 2004; Linding et al., 2004; Rousseau et al., 2006) and AGGRESCAN (Conchillo-Sole et al., 2007) to predict the aggregation-prone segments within T2D-SOD1. The results suggest six aggregation-prone segments exist, including 4-AVCVL-8, 100-EDSVISL-106, and 145-ACGVIGIAQ-153. The aggregation-triggering segments of SOD1 fibril formation have been previously studied (Ivanova et al., 2014). Researchers have solved the atomic structures of two fibril-forming segments from the C terminus, 101-DSVISLS-107 and 147-GVIGIAQ-153, which agrees with our predictions.

Evolutionary pressure on the T2 site and the possible role of kinases: We speculate that SOD1 phosphorylation is a naturally evolved protective mechanism against protein misfolding-induced toxicity. Naturally, one would wonder why SOD1 does not feature aspartic acid at position 2? SOD1 has evolved to be an extremely stable protein, enough so that misfolding-induced disease typically does not manifest itself until post-reproductive age. Hence, evolutionary pressure is insufficient to conserve aspartic acid at position 2. As it becomes more evident that ALS may arise from a synergy of genetic and environmental factors, such as oxidative stress that leads to glutathionylation, having a natural "handle" to mitigate the effects of oxidative modifications may be beneficial to motor neurons. We speculate that SOD1 phosphorylation is catalyzed by a kinase that may be activated under oxidative stress conditions. As a result, the rate of phosphorylation in healthy individuals is approximately 5-6%. Determining phosphorylation rates of SOD1 in ALS patients would be informative for testing this hypothesis. Whether or not the kinase is sensitive to oxidative stress, its malfunction due to genetic mutation may promote SOD1 misfolding and, hence, result in ALS. Therefore, identifying the SOD1 kinase is critically important for potentially identifying genetic markers or modifiers of ALS, as well as for identifying new strategies to combat the disease.

Supplemental References

Conchillo-Sole, O., de Groot, N.S., Aviles, F.X., Vendrell, J., Daura, X., and Ventura, S. (2007). AGGRESCAN: a server for the prediction and evaluation of "hot spots" of aggregation in polypeptides. BMC Bioinformatics *8*, 65.

Fernandez-Escamilla, A.M., Rousseau, F., Schymkowitz, J., and Serrano, L. (2004). Prediction of sequence-dependent and mutational effects on the aggregation of peptides and proteins. Nat. Biotechnol. *22*, 1302-1306.

Ivanova, M.I., Sievers, S.A., Guenther, E.L., Johnson, L.M., Winkler, D.D., Galaleldeen, A., Sawaya, M.R., Hart, P.J., and Eisenberg, D.S. (2014). Aggregation-triggering segments of SOD1 fibril formation support a common pathway for familial and sporadic ALS. Proc. Natl. Acad. Sci. U S A *111*, 197-201.

Khare, S.D., and Dokholyan, N.V. (2006). Common dynamical signatures of familial amyotrophic lateral sclerosis-associated structurally diverse Cu, Zn superoxide dismutase mutants. Proc. Natl. Acad. Sci. U S A *103*, 3147-3152.

Linding, R., Schymkowitz, J., Rousseau, F., Diella, F., and Serrano, L. (2004). A comparative study of the relationship between protein structure and beta-aggregation in globular and intrinsically disordered proteins. J. Mol. Biol. *342*, 345-353.

Proctor, E.A., Fee, L., Tao, Y., Redler, R.L., Fay, J.M., Zhang, Y., Lv, Z., Mercer, I.P., Deshmukh, M., Lyubchenko, Y.L.*, et al.* (2016). Nonnative SOD1 trimer is toxic to motor neurons in a model of amyotrophic lateral sclerosis. Proc. Natl. Acad. Sci. U S A *113*, 614-619.

Rousseau, F., Schymkowitz, J., and Serrano, L. (2006). Protein aggregation and amyloidosis: confusion of the kinds? Curr. Opin. Struct. Biol. *16*, 118-126.